Chemical Engineering Journal 143 (2008) 201–209

Contents lists available at ScienceDirect

Chemical Engineering Journal

journal homepage: www.elsevier.com/locate/cej

Modeling of hydrodynamic cavitation reactors based on orifice plates considering hydrodynamics and chemical reactions occurring in bubble

Amit Sharma, Parag R. Gogate, Amit Mahulkar, Aniruddha B. Pandit*

Chemical Engineering Department, University Institute of Chemical Technology, Nathalal Parikh Marg, Matunga, Mumbai 400019, India

ARTICLE INFO

Article history:
Received 17 August 2007
Received in revised form 18 March 2008
Accepted 10 April 2008

Keywords:
Hydrodynamic cavitation
Bubble dynamics
Chemical reaction
OH radicals
Cavitational yield

ABSTRACT

In the present work, a model has been developed for predicting the cavitational intensity in a hydrodynamic cavitation reactor based on the use of orifice plates considering the hydrodynamic conditions and the different chemical reactions taking place inside the cavity. The model is based on a set of ordinary differential equations and considers the bubble hydrodynamics and heat exchange including the phase change. It also accounts for the chemical reactions of the various gaseous species in the air–water system and diffusion/dissolution of the reaction products from the cavity. Weber number criterion has been incorporated for the stability of the growing bubble. During rapid bubble collapse a large amount of water vapor is trapped inside the bubble, resulting in an increased heat capacity and endothermic chemical reactions leading to lower temperatures at the end of the collapsing event. Analyzing the reaction thermodynamics within the dense, collapsed bubble, it can be said that the effect of excluded volume of the non-ideal gas results in pronounced suppression of the molecule-producing endothermic reactions using Le-Chatelier's principle. Design correlation in terms of cavitational intensity (in terms of collapse pressure and temperatures) and cavitational yield (in terms of OH radicals) aims at understanding the design information related to the dependency of the cavitational intensity and the radical yield on the operating parameters in the case of the hydrodynamic cavitation.

1. Introduction

Cavitation phenomenon resulting into high temperatures and pressures and generation of free radicals has been known to produce spectacular effects in driving chemical reactions [1–4]. Cavitation generated, using hydraulic systems by the passage of liquid through simple geometries such as orifice plate or venturi can also create conditions similar to acoustic cavitation such as enhanced rates of reaction, increase in the catalyst efficiency and has been attempted as an alternative to the acoustic cavitation over the past several years [5,6]. Also, this form of cavitation has been proved to be more efficient for large-scale operation than the acoustic cavitation in several chemical and physical processes such as polymerization and depolymerization of aqueous polymeric solutions [7], fatty oil hydrolysis [8] and microbial cell disruption [9]. In the present work, the hydrodynamic effects of the flow through an orifice, which causes reduction in pressure at vena contracta, and generation of gaseous cavitation bubbles with partial vaporization of cavitating fluid has been discussed. Orifice plate setup has been reported to be highly energy efficient and results in more cavitational effects as compared to the acoustic cavitation-based reactors and also other hydrodynamic cavitation-based reactors such as high-speed and high-pressure homogenizers [1].

The flow model used here for a gas–liquid cavitation reactor considers, the bubble dynamics described by the Keller–Miksis equation [10]. With an aim of approaching realistic situation, the model also considers mass transfer, heat flux, evaporation and condensation of liquid vapor and chemical reactions occurring inside the bubble that leads to altogether 20 first order ordinary differential equations. The final aim of this modeling exercise is to develop design correlations for the prediction of cavitational intensity and chemical effects characterized in terms of cavitational yield. It is important to note here that only reactions which occur inside the cavity have been considered in the present work to quantify the cavitational intensity produced at the time of the collapse. These free radicals when liberated into the liquid bulk will undergo a series of radical reactions including favorable attack towards the chemical substrate present in the system and somewhat unfavorable reactions like recombination reactions producing H_2O_2, HNO_2 and HNO_3. The net cavitational effects will also depend on the conditions existing inside the reactor which will control the diffusion rates and rates of other chemical reactions occurring in the liquid bulk.

* Corresponding author. Tel.: +91 22 24145616; fax: +91 22 24145614.
E-mail address: abp@udct.org (A.B. Pandit).

1385-8947/$ – see front matter © 2008 Elsevier B.V. All rights reserved.
doi:10.1016/j.cej.2008.04.005

Nomenclature

C_1, C_2, C_3	constants in Eqs. (3)–(5)
d_m	maximum stable bubble diameter (m)
d_o	diameter of holes on orifice plate (m)
d_p	diameter of pipe (m)
e	eddy length (m)
f	turbulence frequency (Hz)
OH	maximum amount of OH radicals being formed during the dissociation reaction at the time of collapse
$P_{collapse}$	final collapse pressure (N/m^2)
P_{in}	inlet pressure (atm)
R_0	initial/equilibrium radius of the bubble/cavity (m)
$T_{collapse}$	final collapse temperature (K)
$\bar{v}/$	fluctuating velocity (m/s)
We	Weber number

Greek letters

γ	surface tension of liquid (N/m)
ρ	density of the liquid medium (kg/m^3)

2. Previous work

Neppiras [11] has written an excellent review on the different aspects of the bubble dynamics and is considered one of the basic pioneering works in this field. The modeling of cavitation phenomena has been done over the years with a varied objective ranging from explaining the sonoluminescence of the cavitating bubbles to explaining the effects in the chemical processing applications (Table 1). From the application viewpoint as well as for designing the cavitational reactors, one has to be more interested in the chemical effects of cavitation. The extent of chemical transformations can be correlated to the collapse pressure and/or temperatures generated (for cases where reactions occurs at high temperature) and in terms of the radical generation rates induced by cavitation (for the case where, free radical attack is the controlling mechanism). Various models have been proposed for the quantification of the chemical transformations and to explain the link between the bubble motion and the chemical kinetics. It is important to note that the acceptability of the model as well as the solution schemes strongly depend on the assumptions used in the derivation of the model and the approximations used in the solution schemes. All the earlier models were based on a common platform to explain the variation in the cavity radius with time, i.e. using the conventional Rayleigh Plesset equation of bubble dynamics. A most important disadvantage of this equation, though simple for the solution, was that the equation considers incompressible nature of the medium, which results in the deviations in the predictions of the equation from the realistic situations, particularly at collapse stages where mach number is greater than 1. More recently, the gas dynamics inside collapsing bubbles has been studied considering the compressible Navier–Stokes equations [12,13]. These detailed models have been used to show that the state of the gas on collapse is strongly influenced by processes such as heat transfer, mass transfer, chemical reactions and non-uniform pressure in the bubble interior. This entire set of physical phenomenon has not been included in the traditional Rayleigh–Plesset formulations. The important works in this area [12,14–24] along with the highlights of the work have been depicted in Table 1.

As seen from the table, the earlier works have concentrated mainly on acoustic cavitation-based reactors and try to explain the links between the bubble motion and chemical kinetics. Bubble dynamics in case of hydrodynamic cavitation was earlier simulated by Pandit and co-workers [23,25] but chemical reactions occurring in the cavity was not considered. Also, none of them was directed at systematically exploring the effect of various operating parameters on the cavity radius profiles and hence the final cavitation intensity produced at the collapse of the cavities. The hydrodynamic cavitation reactors are proved to be superior to acoustic cavitation reactors in terms of energy efficiency for given chemical/physical transformation and also in terms of scalability [7–9,26,27]. As said earlier, the present work models the hydrodynamic cavitation reactors and aims at developing an empirical correlation for predicting the pressure generated (measure of the cavitational intensity) as a function of the important operating parameters. The present work considers compressible nature of liquid, chemical reactions occurring inside the cavity and exchange of mass (diffusion and phase change) and heat transfer across the cavity leading to much more realistic situation as compared to the models based on bubble dynamics alone (Rayleigh–Plesset equation). Based on the simulation results, some recommendations regarding the use of optimum operating parameters for maximizing the cavitational effects have been made. It should be also noted here that the current model makes an intrinsic assumption of spherical bubbles in the system which may not be realistic in actual systems and the deformed cavitation bubbles will also be governed by the electric effects. In such a case, equations of Keller and Mikis [10] are not convenient for

Table 1
Brief overview of the important works dealing with bubble dynamics

Models	Important features
Kamath et al. [14]	Separated the chemical kinetics from Rayleigh–Plesset model to predict the production of OH• radicals
Naidu et al. [15]	Simplified model based on Rayleigh–Plesset equation and chemical kinetics to predict OH• radicals generation rate and the effect of parameters such as reactant concentration, temperature, etc.
Yasui [16]	Accounted for chemical reactions and non-equilibrium phase change in collapsing bubble under single bubble sonoluminescence (SBSL) conditions
Sochard et al. [17,18]	Modeled free radicals production in mildly forced bubbles by accounting for non-equilibrium phase change and gas-vapor interdiffusion with Rayleigh–Plesset model
Gong and Hart [19]	Modeled some trends observed in sonochemistry experiments by coupling chemical reactions with Rayleigh–Plesset equation
Colussi et al. [20]	Combined chemical reaction with bubble motion as well as non-equilibrium phase change
Moss et al. [12]	Considered inclusion of water vapor as a cause of various phenomena observed in cavitation-induced bubbles
Storey and Szeri [21]	Accounted for water vapor, chemical reactions, non-equilibrium phase changes, mass and heat transfer as well as radical recombination and used equations of continuity and motion for more realistic picture of bubble/cavity
Moholkar Pandit [23]	Prediction of Bubble dynamics in hydrodynamic cavitation by taking into account the turbulence (heat and mass transfer between cavity and bulk liquid and chemical reaction occurring in the cavity are not considered)
Lohse and Toegel [22]	Bubble dynamics for acoustic cavitation based on chemical reactions occurring in the cavity coupled with heat transfer and mass transfer due to diffusion and phase change
Arrojo and Benito [24]	Bubble dynamics for hydrodynamic cavitation based on Rayleigh–Plesset equation coupled with heat transfer with surrounding liquid (no quantification of OH radicals generated in the cavity)

description of movement of cavitation bubbles in hydrodynamic fields and alternate equations need to be considered, which should form the future work in attaining a more realistic situation. The present work limited by above intrinsic simplifications, however, should be considered as only a first attempt in correct direction to model the hydrodynamic cavitation reactors. The present work quantifies the cavitational intensity generated in the reactors as a function of different operating and geometric parameters with an aim of optimization of the hydrodynamic cavitation reactors. To the best of our knowledge there is no such study for the hydrodynamic cavitation reactors and hence the novelty of the present work is clearly established.

3. The mathematical model

The present mathematical model can be divided into two parts namely bubble dynamics model and turbulence model. The overall bubble dynamics model is similar to that developed for acoustic cavitation by Togel et al. [22]. The bubble dynamics model consists of

1. Keller–Miksis equation of bubble dynamics;
2. Mass transfer models to consider
   (a) phase change of condensable vapor (water vapor) at bubble liquid interface,
   (b) diffusive transfer of non-condensable gases (O^2, N^2, Ar, etc.) at bubble liquid interface,
   (c) change in mass concentration of species due to chemical reactions occurring in the core of cavity.
3. Heat balance equation for modeling conductive and latent heat transfer between cavity and surrounding liquid.

About 45 different chemical reactions taking place in the cavity including dissociative reactions responsible for formation of OH radicals are also considered. Details of the reaction scheme can be obtained from [22]. The model does not consider spatial distribution of concentration of species inside the bubble. But this has been appropriately taken care of by dividing the region inside the bubble into two sections, core and boundary layer, respectively. The boundary layers thickness, for heat and mass transfer, are calculated through out the lifetime of cavity and both the regions are treated separately. This approach greatly reduces the complexity of the problems, which otherwise would have resulted into several partial differential equations thus limiting the practical applicability of the model. It should be noted that such a study of detailed spatial distribution of temperature and concentration inside the cavitation bubble was earlier taken up by Sochard et al. [18]. It was observed that the temperature and concentration profile inside the bubble changes sharply in the boundary layer near the bubble–liquid interface. Thus the bubble could be said to be consisting of hot core and relatively cooler boundary layer at the time of collapse. Thus the approach of dividing the bubble in to two regions, i.e. bubble core and boundary layer is justified as it greatly reduces the mathematical difficulties but still preserves the accuracy of the model.

The turbulence model used here is similar to that developed by Gogate and Pandit [25]. Bubbles produce cavitation conditions when they are excited by external pressure fluctuations. In acoustic cavitation the ultrasound provides these pressure fluctuations while in hydrodynamic cavitation it is turbulent pressure fluctuations near the orifice plate or a venturi that excites the bubble and makes it to produces cavitation conditions. In addition to the turbulence model the bubble stability criterion (Weber number criterion) is also taken in to account. Such a bubble stability criterion was never presented in the earlier literature. In case of acoustic cavitation the cavitation bubbles are generated in almost stagnant liquid, except for liquid streaming occurring near the transducers. The typical liquid velocity generated due to acoustic streaming is of order of 0.5 m/s [28] while the liquid velocities generated in the hydrodynamics cavitation is of order of ~20 m/s, much more than that of acoustic streaming [8,9]. Thus the turbulent shear acting on bubble in hydrodynamic cavitation is much higher than that occurring in acoustic cavitation. Thus it is very necessary to consider the bubble stability in case of hydrodynamic cavitation. Weber number criterion restricts the maximum size that could be attained by the bubble. It will be seen in later section that the maximum size attained by the bubble dominantly decides the amount of water vapor present in the cavity and hence the number of OH radicals generated in the cavity. Thus Weber number criterion greatly changes the bubble dynamics which otherwise would have been similar to that of acoustic cavitation. The turbulence model predicts the turbulence pressure fluctuations that are generated due to flow of liquid in the downstream of the orifice. This model considers all the geometrical parameters like diameter and number of holes on orifice plate, diameter of pipe and operating parameters like liquid velocity at the orifice, inlet pressure and downstream pressure for calculation of turbulence pressure fluctuations.

3.1. Stability criterion for bubbles

The stability of gas bubbles in a turbulent liquid of low viscosity is of crucial importance in many processes involving gas–liquid reactions. In the present work, the critical Weber number criteria for the stability of the growing bubble has been used. From an earlier work [29] it has been suggested that in a turbulent liquid, maximum stable bubble diameter (d_m) is determined by the Weber number

$$We = \frac{\rho\, v'^2 d}{\gamma} \tag{1}$$

where v'^2 is the turbulent fluctuating velocity, d is bubble diameter, ρ and γ are liquid density and surface tension, respectively. This dimensionless group is proportional to the ratio of (i) the inertial force, which deforms the bubble, to (ii) the surface tension force, which stabilizes the bubble. The bubble will split if Weber number (We) is greater than critical Weber number ($We_c = 4.7$). Thus maximum size of bubble is given by

$$d_m = \frac{4.7\,\gamma}{\rho\, v'^2} \tag{2}$$

When solving the Keller–Miksis equation (5), the Weber number criterion is being applied at every stage during the bubble life. If size of the bubble exceeds the maximum allowed size (based on Weber number criterion) the bubble size is equated to maximum size given by (2).

4. Results and discussion

Simulations were carried out to find out the cavity/bubble behavior under hydrodynamic cavitation conditions. The effects of the different operating parameters on the bubble behavior and in turn on the cavitational intensity have been elucidated.

4.1. Effect of chemical reaction on bubble dynamics

In this section we discuss the effect on bubble dynamics of consideration of chemical reaction occurring in the bubble. Fig. 1 shows cavity dynamics of 1, 10 and 40 μm of initial size of nuclei when chemical reactions occur in the cavity and when chemical reactions

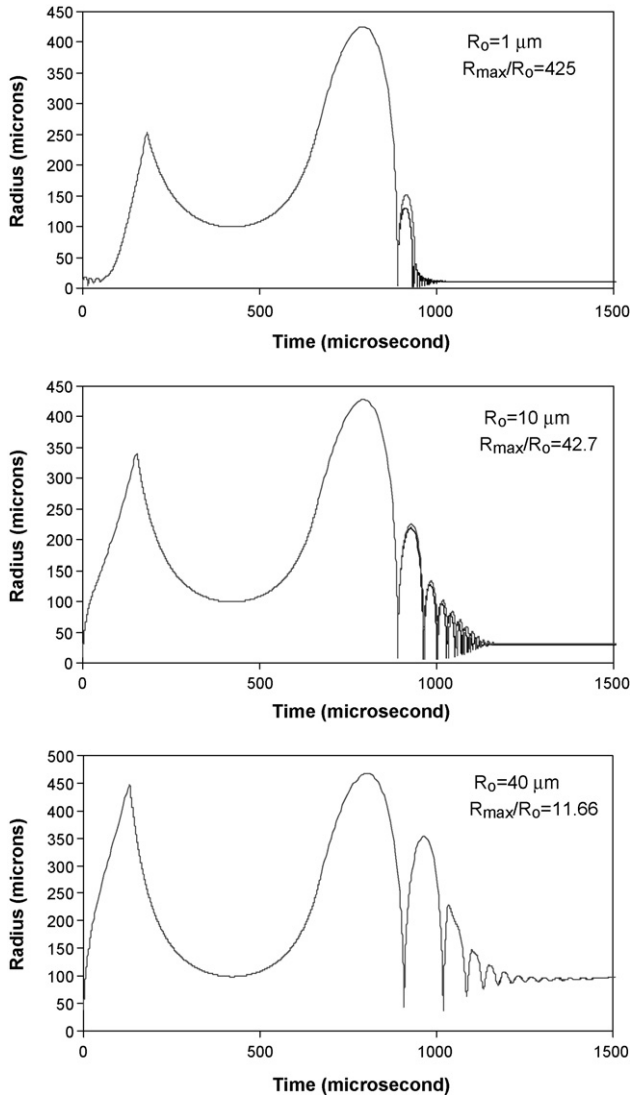

Fig. 1. Radius history for different initial sizes of nuclei in the presence and absence of chemical reactions. P_{in} = 3 atm; temperature = 298 K; dia orifice/dia pipe = 0.1; dia pipe = 5 cm; cavitation number = 0.6.

do not occur in the cavity while subjecting them to same cavitational conditions (P_{in} = 3 atm, Pipe dia. = 50 mm, orifice dia. = 5 mm, number of holes = 4, orifice velocity = 23 m/s). One should note that when we say the chemical reactions are not considered to occur in the cavity, it means that the mass of chemical species present inside the cavity does not change due to chemical reactions, but cavity exchanges mass with the bulk liquid either by evaporation/condensation of water and/or by diffusion of non-condensable gases from/into the cavity. It is seen from Fig. 1 that for all the cases of initial size of nuclei the radius history is not much affected by inclusion or exclusion of chemical reactions in the cavity. Table 2 shows the collapse pressure and temperature obtained for 1, 10 and 40 μm nuclei for cavity dynamics with and without chemical reaction. It is seen that, although the bubble dynamics is not affected by chemical activity of the cavity, but the collapse pressure and temperature is greatly affected by it. Especially the collapse temperature is seen to be much lower when chemical reactions occur in the cavity. This is clearly because of the endothermic dissociation reactions occurring in the cavity during its collapse phase. The values of collapse pressure are seen to be higher when chemical reactions are considered to occur in the cavity. This is because of

Table 2
Effect of chemical reaction on collapse pressure and temperature generated inside the cavity of different initial sizes

Initial size of cavity	Collapse pressure (atm)		Collapse temperature (K)	
	With reaction	Without reaction	With reaction	Without reaction
1	14,094	3341	7816.5	53461.4
10	4,411	4078	4396.85	5197.06
40	95	95	1845.03	1845.03

increase in number of molecule generated from dissociation reactions during the collapse phase of the cavity. Thus it can be seen from above simulations that the bubble dynamics is not affected by chemical reaction taking place in the cavity. Hence for cavitation assisted physical transformation like nanoparticle synthesis, crystallization, emulsification, microbial cell disruption where the turbulence and high velocity liquid jets produced by the cavity is to be estimated, chemical reaction can be neglected from cavity dynamic model. For cavitation-assisted chemical transformation like waste treatment (oxidation) and chemical synthesis, where it is necessary to quantify the OH radical produced from a cavity chemical reactions occurring in the cavity should be included in cavity dynamics models.

Fig. 2 (primary *Y*-axis) shows the molecular concentration (mol/m^3) of water in the cavity. It is seen that the concentration of water molecules remains fairly constant (partial pressure of water is equal to vapor pressure of water) throughout the life time of cavity indicating that the evaporation and condensation of water is much faster than the bubble dynamics except at the collapse stages of the cavity. At collapse stage the mass and heat transfer ceases but molar concentration of water vapor increases due to adiabatic compression. Thus the bubble is saturated with water for most of the part of its life. From Fig. 2 (secondary *Y*-axis) it is seen that the number of molecules of O_2 and N_2 in the cavity remains almost constant indicating that the diffusion of gases from/into the bubble is rather slow process. However, at the time of collapse due to increased pressure some small amount of non-condensable gases diffuse out of the bubble into the liquid.

Fig. 3 shows the number of OH radicals generated in 10 μm nuclei during is life time. It is seen that OH radicals are generated only during the collapse phase of the cavity when pressure and temperature in cavity is sufficiently high to promote dissociation reactions. Once the OH radicals are generated they start oxidizing other chemical species present in the cavity. It can also be seen that the amount of OH radical produced per collapse goes on reducing with reduction in magnitude of collapse pressure. This reduction in number of OH radical produced in subsequent partial collapse can also be because of lesser number of water molecules present in the

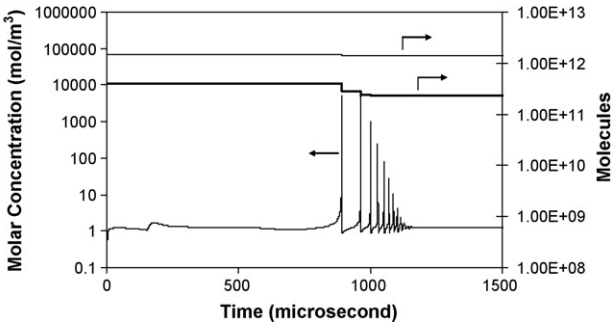

Fig. 2. Molar concentration of water (primary *Y*-axis) and molecules of oxygen and nitrogen in cavity (secondary *Y*-axis). P_{in} = 3 atm; temperature = 298 K; dia orifice/dia pipe = 0.1; dia pipe = 5 cm; cavitation number = 0.6.

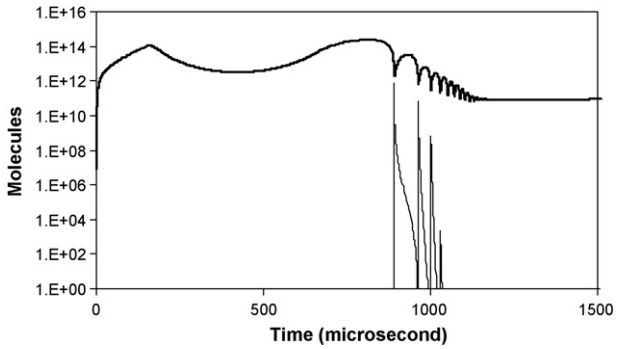

Fig. 3. Water molecules and OH radicals generated in cavity. P_{in} = 3 atm; temperature = 298 K; dia orifice/dia pipe = 0.1; dia pipe = 5 cm; cavitation number = 0.6.

cavity because the maximum size attained by cavity reduces in each subsequent cycle. In next section correlation to predict the amount of OH radicals generated will be proposed based on operating and geometrical parameters of the cavitation device.

4.2. Effect of initial bubble radius

The study by Moholkar and Pandit [30]; have indicated that it is necessary to assess the dynamics of bubbles of all sizes in a similar environment and as both collapse pressure pulses and bubble sizes significantly depend upon the initial radius, the typical size range of the bubbles 1–50 μm have been considered in this work. It is also worth noting here that, in most practical systems involving high-energy cavitation (such as those involving sonochemical, biological and erosive effects), the bubbles do not behave as the isolated entities modeled by this single-bubble theory and the cavitational effect may be dominated by the characteristics of the entire bubble population, which may influence, and be influenced by, the cavitational field. More details about the bubble population concept can be obtained from the earlier work of Leighton [31]. As a starting point, single bubble theory has been used in the present work for modeling of hydrodynamic cavitation reactors.

Though it is difficult to exactly control the initial size of nuclei in an actual hydrodynamic reactor, manipulating the liquid physicochemical properties and presence of dissolved species can give some indication of the initial size. The variation in the radius with time and the conditions of the simulation has been shown in Fig. 1 for initial cavity radius of 1, 10, and 40 μm. The ratio of the maximum radius to the initial radii during oscillations is higher for smaller bubbles. It is seen in all the radius history profiles (Fig. 1) that the bubble undergoes sudden shrinkage in its growth phase. As the bubble expands in high velocity liquid jet near orifice, more and more turbulent shear acts on the bubble which causes it to split due to the critical Weber number criterion. The maximum value that a bubble could attain is greatly controlled by local turbulence. Thus R_{max}/R_0 decreases with an increase in the initial radius. The variation in the collapse temperature and collapse pressure pulse with initial radius of the cavity and the conditions has been shown in Fig. 4(a and b). It can be clearly seen that the pressure and temperature pulse generated at the time of the collapse decreases with an increase in the initial radius of the nuclei, since the magnitudes of the pressure pulse produced by these bubbles during the collapse are proportional to the ratio of the maximum radius to that of initial bubble radius before the collapse occurs.

Also, since different sizes of bubbles attains same maximum radius (due to the Weber number restriction), the maximum amount of water present at the time of maximum expansion (R_{max}) are equal, therefore OH radicals produced at the time of collapse of

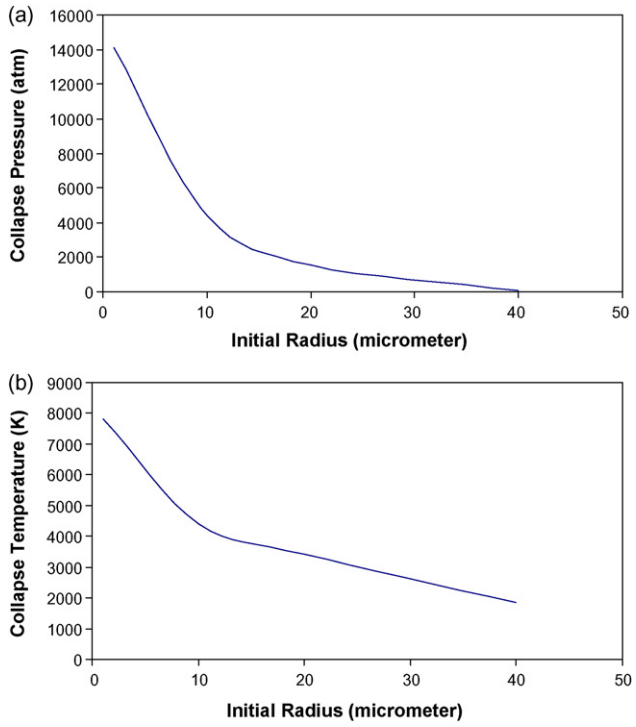

Fig. 4. (a and b) Variation of collapse pressure and temperature with initial radii. P_{in} = 3 atm; temperature = 298 K; dia orifice/dia pipe = 0.1; dia pipe = 5 cm; cavitation number = 0.6.

cavity also remains almost same with the variation in the initial radii (Fig. 5). It is difficult to give the exact nuclei size that will be generated in the reactor during the cavitation phenomena and hence direct verification of the obtained trends with experimental results is not possible. However, some trends can be obtained depending on the medium vapor pressure and the presence of the dissolved gases in the medium. As the vapor pressure of the medium increases, the size of the bubble or cavity, which will be formed, will increase at otherwise similar operating conditions, resulting into a decrease in the magnitude of the pressure pulse generated. Mujumdar and Pandit [32] have indicated a decrease in the yield of fumaric acid with an increase in the medium vapor pressure obtained by using ethanol–water mixtures. Senthil Kumar et al. [6] have also indicated, using experiments on degradation of KI in a 50-L hydrodynamic cavitation setup with different orifice plates, that the degradation rates are much larger during the initial stages of treatment when dissolved gases were present in the system.

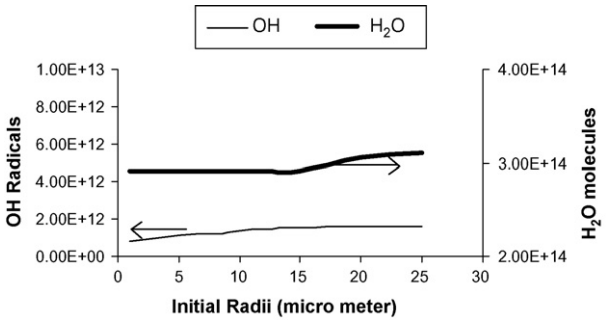

Fig. 5. Amount of OH• and H_2O varying with initial radii. P_{in} = 3 atm; temperature = 298 K; dia orifice/dia pipe = 0.1; dia pipe = 5 cm; cavitation number = 0.6.

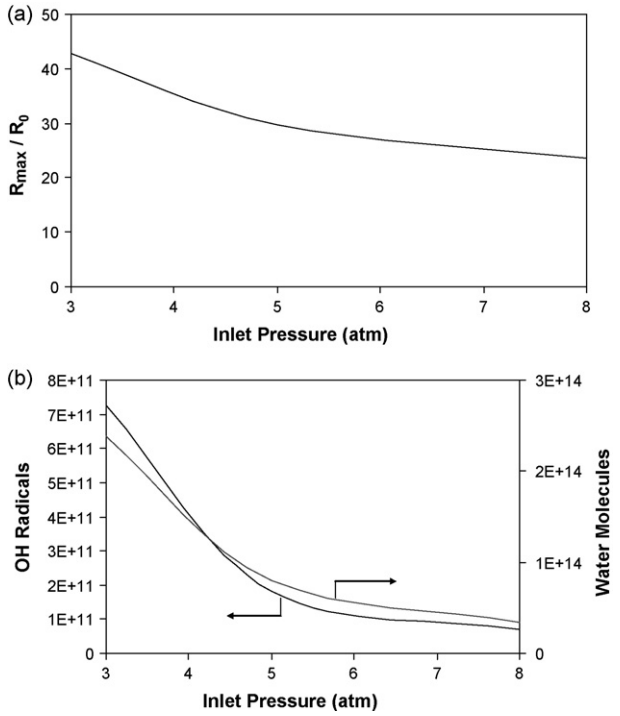

Fig. 6. (a and b) Ratio of maximum size attained by the cavity to initial size (R_{max}/R_0) and the amount of OH• and H_2O varying with inlet pressure. R_0 = 1 μm; temperature = 298 K; dia orifice/dia pipe = 0.1; dia pipe = 5 cm; cavitation number = 0.6.

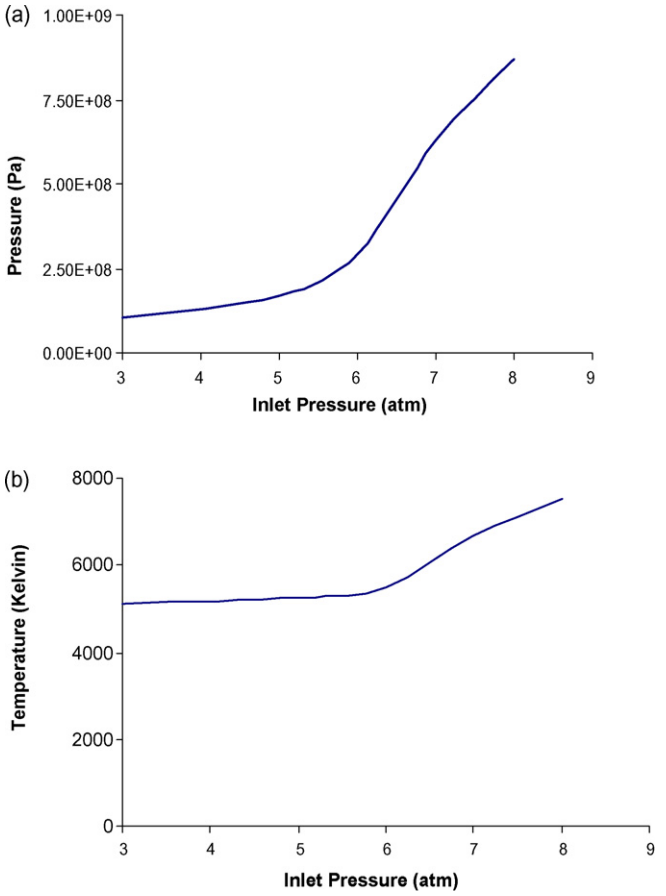

Fig. 7. (a and b) Variation of collapse pressure and temperature with inlet pressure. R_0 = 1 μm; temperature = 298 K; dia orifice/dia pipe = 0.1; dia pipe = 5 cm; cavitation number = 0.6.

4.3. Effect of inlet pressure

Simulations were carried out to examine the effect of inlet pressure on the cavity radius history and the magnitude of pressure pulses resulting from the collapse of the cavitational bubble. The inlet pressure into the system was varied in the range 3–8 atm. The intensity of the collapse of the cavity depends mainly on the rate of change of turbulent pressure in the downstream section of the orifice and the final magnitude of the recovered pressure downstream of the orifice. Increase in the orifice upstream pressure, increases the downstream pressure (provided it does not discharge to atmosphere), liquid flowrate and also the energy dissipation rate into the system resulting into a higher permanent pressure drop across the orifice and increased power input per unit mass of liquid.

Due to an increase in the fluctuating velocity (v') with increase in the power input per unit mass of the liquid, the maximum radius that could be attained by the cavity decreases (Weber number criteria). Also, the dynamics of the bubble changes with the inlet pressure, as growth is restricted and shows a decreasing trend in the maximum growth with an increasing inlet pressure (Fig. 6a).

The number of molecules of water influx during the expansion depends on the maximum radius attained. We can observe a decreasing trend in the maximum number of H_2O molecules with an increase in the inlet pressure (Fig. 6b) and which in turn decreases the amount of OH radicals being formed during the dissociation reaction at the time of collapse.

The variation in the collapse pressure and temperature pulses with the inlet pressure and the conditions of the simulations has been depicted in Fig. 7(a and b). The quantum of the total collapse pressure (collapse pressure due to a single cavity *X* number of cavities) can decrease beyond a certain inlet pressure, as the effect of the number of cavities will be more pronounced. Thus there is an optimum inlet pressure that should be used for getting the maximum benefits from the system (where there is a condition that the flow rate must be kept constant). Experimental studies on cell disruption using the orifice plate indicate that the percentage of cell breakage increases with the operating pressure up to a point and then decreases [33]. Similar results were obtained for the high-pressure homogenizer [26]. Experimental studies using aqueous KI decomposition as a model reaction also shows that such an optimum pressure does exist at which the iodine liberation is maximum [2,34].

4.4. Effect of orifice to pipe diameter ratio

Simulations were carried to find out the dependence of bubble behavior on the orifice diameter. However, it should be kept in mind that when ratio of diameters is varied, liquid velocity for given pressure drop across will change. For simulation purpose change in liquid velocity at orifice and inlet pressure in not considered and thus results discussed here is representative of change in variation in diameter ratios rest while maintaining rest of the parameters. Increase in the orifice to pipe diameter ratio (d_o/d_p), increases the power input per unit liquid volume that further increases the fluctuating velocity (v') and finally the frequency of turbulence ($f = v'/e$) also increases. Higher frequency of turbulence restricts the maximum radius attained by the cavity (Weber no. Criteria) and hence the maximum radius reached by the bubble during its growth phase decreases. The conditions and result of simulation (maximum radius attained by the cavity) are shown in Fig. 8(a). Also with the decrease in the maximum radius of the cavity, the number of H_2O molecules and OH radicals gives a decreasing trend (Fig. 8b) due to the reason explained earlier.

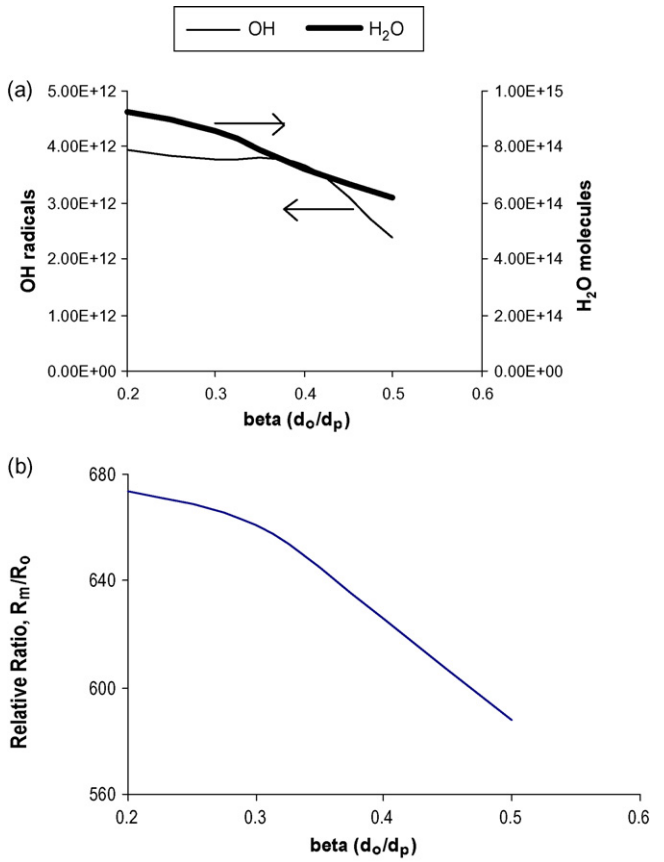

Fig. 8. (a and b) The amount of OH• and H_2O molecules and the Ratio of maximum size attained by the cavity to initial size (R_{max}/R_0) varying with orifice to pipe diameter ratio. R_0 = 1 μm; temperature = 298 K; P_{in} = 3 atm; cavitation number = 0.6.

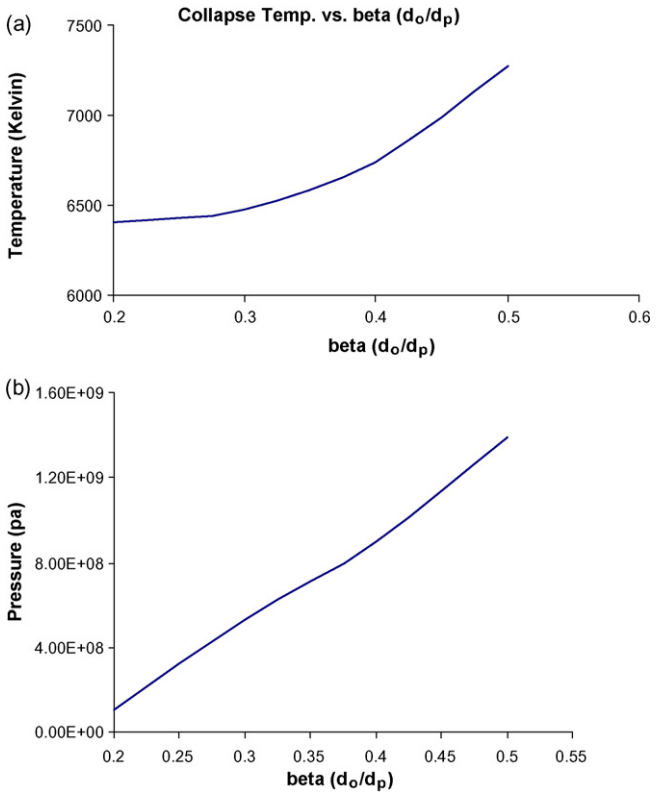

Fig. 9. (a and b) Variation of collapse temperature and pressure with orifice to pipe diameter ratio. R_0 = 1 μm; temperature = 298 K; P_{in} = 3 atm; cavitation number = 0.6.

It can be seen from Fig. 9(a and b) that as the diameter of the orifice hole increases, the collapse pressure generated also increases. This can be attributed to the variation of the cavitation inception number as well as operating cavitation number with the diameter of the orifice hole. Yan and Thorpe [35] have shown that the cavitation inception number (cavitation number for the onset of cavitation), increases with an increase in the diameter of the orifice hole. Also, operating cavitation number will increase with an increase in the diameter of the hole. Thus, as long as the extent of increase in cavitation number is below the extent of increase in the cavitation inception number, the extent of cavitation increases for the same cavitation number with an increase in the orifice diameter. The numerical scheme does indicate this variation correctly, and it is also confirmed by the experiments performed on the hydrodynamic cavitation setup using the model reaction of KI decomposition [36] for an operating cavitation number range of 0.05–2.

5. Development of design correlations

The collapse pressure and temperature is found to be a function of the various operating parameters (inlet pressure, diameter of orifice hole, initial radii), which in turn can be related, with the yield of hydroxyl radicals during the cavity collapse and number of water molecules during the expansion. A bubble pulsating in the water containing dissolved air is thought to contain primarily argon, because the nitrogen, oxygen and water molecules diffuse into the bubble during the expansion react to form soluble products during the bubble compression and the collapse. Thus, the expected initial products of chemical reactions inside the bubble include OH radicals. In the present work we have estimated the yield of OH radical under different conditions and can propose a correlation between yields of the OH radicals and the collapse pressure and temperature with inlet pressure, the diameter of the orifice hole and the initial radius of the nuclei, which can be used to correlate the chemical products formed.

The variation in the collapse pressure and collapse temperature with initial cavity radius, inlet pressure and the ratio of diameter of the orifice hole to the pipe diameter has been represented in Figs. 4, 7 and 9, respectively. Mathematical dependency has been established for this variation and the correlations are proposed as

$$P_{collapse} = C_1 \left\{ R_0^{-1.2402} \times P_{in}^{2.1949} \times \left(\frac{d_o}{d_p} \right)^{-0.4732} \right\} \quad (3)$$

$$T_{collapse} = C_2 \left\{ R_0^{-0.2877} \times P_{in}^{0.3579} \times \left(\frac{d_o}{d_p} \right)^{0.1303} \right\} \quad (4)$$

$$OH = C_3 \left\{ R_0^{0.2428} \times P_{in}^{-4.6457} \times \left(\frac{d_o}{d_p} \right)^{-0.4732} \right\} \quad (5)$$

where $P_{collapse}$ is the final collapse pressure in Pascal (N/m^2), R_0 is the initial radius in μm, P_{in} is the inlet pressure in atm and d_o/d_p is the orifice to pipe diameter ratio and the above correlation is developed over the following range of operating parameters, which are commonly used in the hydrodynamic cavitation applications.

Initial cavity size = 1–50 μm.
Inlet pressure = 3–8 atm.
Ratio of orifice to pipe diameter ratio = 0.2–0.5.

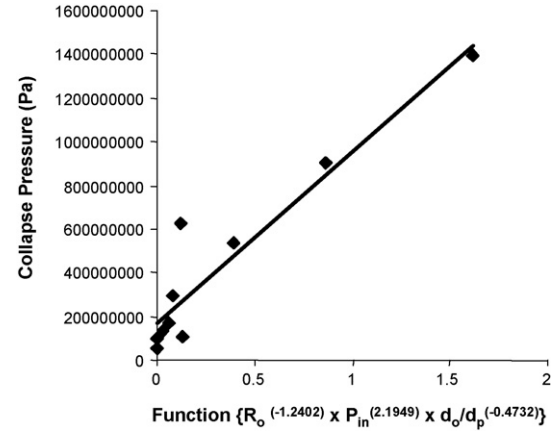

Fig. 10. Variation of collapse pressure with the function at R.H.S. of Eq. (3).

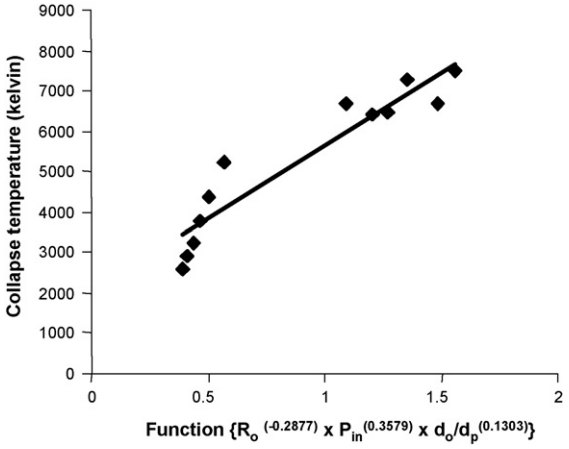

Fig. 11. Variation of collapse temperature with the function at R.H.S. of Eq. (4).

To calculate the constants C_1, C_2, C_3 the mathematical relationship has been established and a linear plot of the $P_{collapse}$, $T_{collapse}$ and OH radicals are plotted against their respective function Eqs. (3)–(5) shown in Figs. 10–12, respectively. The values of constants C_1, C_2, C_3 have been obtained to be equal to 8×10^8, 3633.3 and 4.0×10^{13}, respectively.

The development of correlation is based on results obtained from the solution of the theoretical equations used in the modeling explained before and hence gives a realistic approach. Thus, can be said that the correlation can be used for the design of a hydrodynamic cavitation setup using a orifice plate in a pipe as a cavitating device.

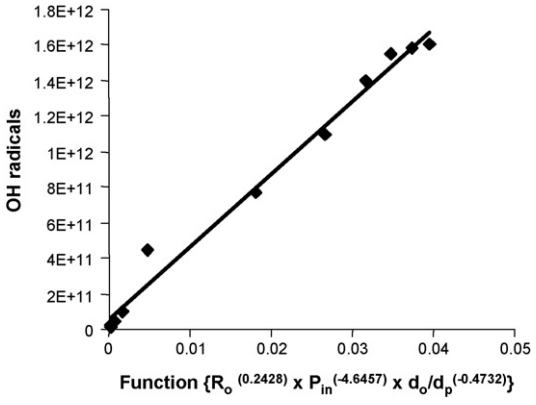

Fig. 12. Variation of OH radicals with the function at R.H.S. of Eq. (5).

6. Conclusions

The present work reports numerical simulation of the bubble dynamics in hydrodynamic cavitation reactors. Critical Weber number criterion for the stability of the growing bubble is used in the present work. The parameters such as orifice diameter to pipe diameter ratio, initial radius and inlet pressure has been found to affect the bubble behavior (maximum radius reached by the cavity and the magnitude of the collapse pressure pulse).

It is seen that the bubble dynamics is not affected by chemical reactivity of the content of cavity, but the collapse conditions, i.e. collapse temperature and pressure are greatly altered by chemical reactions taking place in the cavity. During the collapse phase, water vapor and/or any other chemical species present in the cavity are subjected to extreme conditions of temperature and pressure. Under these conditions, the chemical species decompose generating free radicals. Account of the two opposing effects due to the endothermic nature of major reactions in the presence of water vapor and the relevance of Le Chatelier's principle applied to a reactive van der Waals gas has been taken into consideration.

Correlations has been developed for the prediction of the magnitude of the pressure and temperature pulse generated by the collapse of the cavity and maximum amount of OH radicals generated during collapse as a function of initial cavity size, diameter of orifice hole and inlet pressure. The correlation considers the effect of bubble hydrodynamics with heat flux, phase change of water by evaporation and condensation of vapor, chemical reactions of the various gaseous species in the bubble and diffusion or dissolution of the reaction products in the liquid. The developed correlation can be helpful in the selection of suitable parameters for an optimum design of the hydrodynamic cavitation reactor, depending on the desired chemical or physical transformation.

Acknowledgements

Authors would like to acknowledge the funding of Department of Science and Technology, for the project and one of the authors (A.S.) would also gratefully like to acknowledge the financial support from UGC (University Grants Commission), India for the fellowship.

References

[1] P.R. Gogate, I.Z. Shirgaonkar, M. Sivakumar, P. Senthilkumar, N.P. Vichare, A.B. Pandit, Cavitation reactors: efficiency analysis using a model reaction, AIChE J. 47 (2001) 2526–2538.
[2] I.Z. Shirgaonkar, A.B. Pandit, Degradation of aqueous solution of potassium iodide and sodium cyanide in presence of carbon tetrachloride, Ultrason. Sonochem. 4 (1997) 245.
[3] A. Francony, C. Petrier, Sonochemical degradation of carbon tetrachloride in aqueous solution at two frequencies: 20 kHz and 500 kHz, Ultrason. Sonochem. 3 (1996) S77.
[4] P.R. Gogate, S. Mujumdar, J. Thampi, A.M. Wilhelm, A.B. Pandit, Destruction of phenol using sonochemical reactors: scale up aspects and comparison of novel configuration with conventional reactor, Sep. Purif. Technol. 34 (2004) 25.
[5] V.S. Moholkar, A.B. Pandit, Modeling of hydrodynamic cavitation reactors: a unified approach, Chem. Eng. Sci. 56 (2001) 6295.
[6] P. Senthil Kumar, M. Sivakumar, A.B. Pandit, Experimental quantification of chemical effects of hydrodynamic cavitation, Chem. Eng. Sci. 55 (2000) 1633.
[7] M.M. Chivate, A.B. Pandit, Effect of sonic and hydrodynamic cavitation on aqueous polymeric solutions, Ind. Chem. Eng. 35 (1993) 52.
[8] J.B. Joshi, A.B. Pandit, Hydrolysis of fatty oils: effect of cavitation, Chem. Eng. Sci. 48 (1993) 3440.
[9] S.S. Save, J.B. Joshi, A.B. Pandit, Microbial cell disruption in hydrodynamic cavitation, Chem. Eng. Res. Des 75C (1997) 41.
[10] J.B. Keller, M. Miksis, Bubble oscillations of large amplitude, J. Acous. Soc. Am. 68 (1980) 628.

[11] E.A. Neppiras, Acoustic cavitation, Phys. Rep. 61 (1980) (1980) 159.
[12] W.C. Moss, D.A. Young, J.A. Harte, J.L. Levatin, B.F. Rozsnyai, G.B. Zimmerman, I.H. Zimmerman, Computed optical emissions from sonoluminescing bubble, Phys. Rev. E 59 (1999) 2986.
[13] B.D. Storey, A.J. Szeri, Mixture segregation within sonoluminescence bubbles, J. Fluid Mech. 396 (1999) 203.
[14] V. Kamath, A. Prosperetti, F.N. Egolfopoulos, A theoretical study of sonoluminescence, J. Acous. Soc. Am. 94 (1993) 248.
[15] D.V. Naidu, R. Rajan, K.S. Gandhi, R. Kumar, S. Chandrasekaran, V.H. Arakeri, Modelling of batch sonochemical reactor, Chem. Eng. Sci. 49 (1994) (1994) 877.
[16] K. Yasui, Alternative model of single-bubble sonoluminescence, Phys. Rev. E 56 (1997) 6750.
[17] S. Sochard, A.M. Wilhem, H. Delmas, Modeling of free radical production in a collapsing gas-vapour bubble, Ultrason. Sonochem. 4 (1997) 77.
[18] S. Sochard, A.M. Wilhelm, H. Delmas, Gas vapour bubble dynamics and homogenous sonochemsitry, Chem. Eng. Sci. 53 (1998) 239.
[19] C. Gong, D.P. Hart, Ultrasound induced cavitation and sonochemical yields, J. Acous. Soc. Am. 104 (1998) 2675.
[20] A.J. Colussi, L.K. Weavers, M.R. Hoffmann, Chemical bubble dynamics and quantitative sonochemistry, J. Phys. Chem. A 102 (1998) 6927.
[21] B.D. Storey, A.J. Szeri, Water vapour, sonoluminescence and sonochemistry, Proc. R. Soc. Lond. A 456 (2000) 1684.
[22] R. Togel, S. Hilgenfeldt, D. Lohse, Suppressing dissociation in sonoluminescing bubbles: the effect of excluded volume, Phys. Rev. Lett. 88 (2002) 34301.
[23] V.S. Moholkar, A.B. Pandit, Bubble behavior in hydrodynamic cavitation: effect of turbulence, AIChE J. 43 (1997) 1641.
[24] S. Arrojo, Y. Benito, A theoretical study of hydrodynamic cavitation, Ultrason. Sonochem. 15 (2008) 203–211.
[25] P.R. Gogate, A.B. Pandit, Engineering design methods for cavitation reactors. II. Hydrodynamic cavitation, AIChE J. 46 (8) (2000) 1641–1649.
[26] S.T.L. Harrison, A.B. Pandit, The disruption of microbial cells by hydrodynamic cavitation, in: International Biotechnology Symposium, Washington, DC, USA, 1992.
[27] K.K. Jyoti, A.B. Pandit, Effect of cavitation on chemical disinfection efficiency, Water Res 38 (2004) 2248–2257.
[28] N.P. Vichare, P.R. Gogate, V.Y. Dindore, A.B. Pandit, Mixing time analysis of a sonochemical reactor, Ultrason. Sonochem. 8 (2001) 23–33.
[29] J.O. Hinze, Fundamentals of the hydrodynamic mechanism of splitting in dispersion processes, AIChE J. 1 (1955) 289.
[30] V.S. Moholkar, A.B. Pandit, Harness cavitation to improve processing, Chem. Eng. Prog. 9 (1996) 57.
[31] T.G. Leighton, Bubble population phenomena in acoustic cavitation, Ultrason. Sonochem. 2 (1995) S123.
[32] S. Mujumdar, A.B. Pandit, Emulsification by ultrasound, relation between intensity and ultrasound quantity, Ind. J. Chem. Tech. 4 (1998) 277–284.
[33] L.C. Gareth, E.I. Danver, The disruption of microbial cells by hydrodynamic and ultrasonic cavitation, Project Report, University of Cape Town, Cape Town, South Africa, 1996.
[34] I.Z. Shirgaonkar, Effect of ultrasonic irradiation on chemical reactions, PhD Thesis, University of Mumbai, Mumbai, India, 1997.
[35] Y. Yan, R.B. Thorpe, Flow regime transitions due to cavitation in flow through an orifice, Int. J. Multiphase Flow 16 (1990) 1023.
[36] N.P. Vichare, P.R. Gogate, A.B. Pandit, Optimization of hydrodynamic cavitation using a model reaction, Chem. Eng. Tech. 23 (2000) 683–690.